Combined magnetic ligand fishing and high-resolution inhibition profiling for identification of α-glucosidase inhibitory ligands: A new screening approach based on complimentary inhibition and affinity profiles.

Sileshi G. Wubshet[a,b 1], Bingrui Liu[a,c,d 2], Kenneth T. Kongstad[a 3], Ulrike Böcker[b 4], Malene J. Petersen[a], Tuo Li[a], Junru Wang[d5], Dan Staerk[a,*6]

[a]*Department of Drug Design and Pharmacology, Faculty of Health and Medical Sciences, University of Copenhagen, Universitetsparken 2, DK-2100 Copenhagen, Denmark*

[b]*Nofima AS-Norwegian Institute of Food, Fisheries and Aquaculture Research, PB 210, N-1431 Ås, Norway*

[c]*College of Chemistry and Technology, Hebei Agricultural University, Huanghua 061100, China*

[d]*College of Science, Northwest Agriculture and Forest University, Yangling 712100, China*

E-mail addresses: sileshi.wubshet@nofima.no (S.G. Wubshet)

jiajia912710@hotmail.com (B. Liu)

kenneth.kongstad@sund.ku.dk (K.T. Kongstad)

ulrike.bocker@nofima.no (U. Böcker)

mjp@sund.ku.dk (M.J. Pedersen)

tuo.li@sund.ku.dk (T. Li)

wangjunru@nwsuaf.edu.cn (J. Wang)

[1] 0000-0001-7423-4043
[2] 0000-0001-9243-4217
[3] 0000-0003-4487-7886
[4] 0000-0001-5443-9340
[5] 0000-0003-1967-5967
[6] 0000-0003-0074-298X

ds@sund.ku.dk (D. Staerk).

*Corresponding author at: Department of Drug Design and Pharmacology, Faculty of Health and Medical Sciences, University of Copenhagen, Universitetsparken 2, DK-2100 Copenhagen, Denmark

Graphical Abstract:

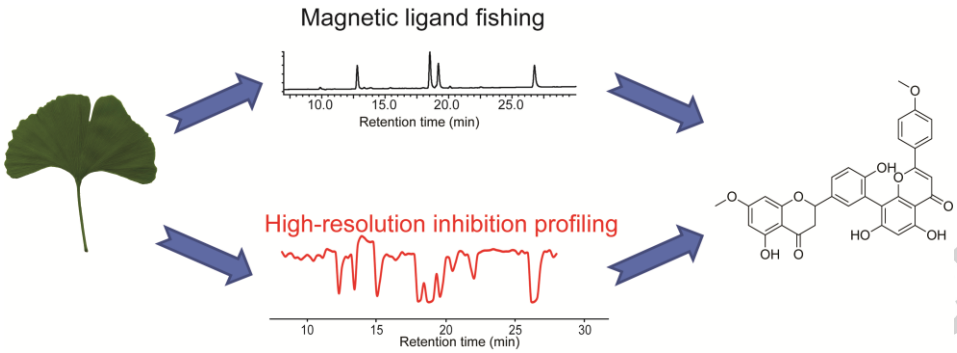

Keywords:

Ligand fishing; High-resolution inhibition profiling; α-Glucosidase; *Ginkgo biloba*

Abstract

Plants are well-recognized sources of inhibitors for α-glucosidase - a key target enzyme for management of type 2 diabetes. Recently, two advanced bioactivity-profiling techniques, *i.e.*, ligand fishing and high-resolution inhibition profiling, have shown great promises for accelerating identification of α-glucosidase inhibitors from complex plant extracts. Non-specific affinities and non-specific inhibitions are major sources of false positive hits from ligand fishing and high-resolution inhibition profiling, respectively. In an attempt to minimize such false positive hits, we describe a new screening approach based on ligand fishing and high-resolution inhibition profiling for detection of high-affinity ligands and assessment of inhibitory activity, respectively. The complementary nature of ligand fishing and high-resolution inhibition profiling was explored to

identify α-glucosidase inhibitory ligands from a complex mixture, and proof-of-concept was demonstrated with crude ethyl acetate extract of *Ginkgo biloba*. In addition to magnetic beads with a 3-carbon aliphatic linker, α-glucosidase was immobilized on magnetic beads with a 21-carbon aliphatic linker; and the two different types of magnetic beads were compared for their hydrolytic activity and fishing efficiency.

1. Introduction

Modern analytical techniques, such as HPLC, LC-HRMS and HPLC-PDA-HRMS-SPE-NMR, provide fast identification and/or full structural characterization of constituents in complex mixtures. However, none of these techniques provide information about the constituents' bioactivity, and there is a great need for fast and robust analytical-scale techniques that can pinpoint individual bioactive constituents in complex mixtures. High-resolution inhibition profiling and ligand fishing are two recent bioactivity-profiling techniques that have shown great promises for successful natural product-based drug discovery [1,2]. In high-resolution inhibition profiling, fractions collected from analytical-scale HPLC separation are subjected to microplate-based bioassaying to provide a high-resolution inhibition profile (biochromatogram). These profiles can be used to guide subsequent isolation and identification towards bioactive constituents. In combination with HPLC-PDA-HRMS-SPE-NMR or targeted preparative-scale isolation, this technique has been used for identification of α-glucosidase inhibitors, α-amylase inhibitors, monoamine oxidase-A inhibitors, antioxidants, and fungal plasma membrane H^+-ATPase inhibitors from endophytes and plants [3-7].

In ligand fishing, a target enzyme immobilized on a solid support is used to 'fish' out potential ligands from a complex mixture. The ligand-containing fraction eluted from the immobilized enzyme can subsequently be subjected to chromatographic analysis to provide a chemical profile of ligands with affinity to the immobilized target enzyme. These ligands can be structurally characterized either directly from the ligand-containing fraction using LC-HRMS or through

targeted HPLC-PDA-HRMS-SPE-NMR analysis of crude extract [8-9]. Ligand fishing based on magnetic nanoparticles has been demonstrated as an excellent tool for identification of bioactive constituents in plant extracts [9-12].

The major advantage with both high-resolution inhibition profiling and ligand fishing techniques, is the possibility of detecting bioactive constituents directly from crude extracts without any pre-purification procedures. However, the two techniques are governed by two different, and in some cases complementary, principles. For example, in the case of α-glucosidase, bioactivity profiles from ligand fishing are based on binding affinity of molecules to the enzyme regardless of their inhibitory potential. However, non-specific affinity of a molecule towards the immobilized enzyme or the solid support is a common source of false positive results in ligand fishing. High-resolution α-glucosidase inhibition profiling provides a measure of the inhibitory potential of the bioactive molecules, but even though the binding affinity of a ligand towards the catalytic pocket is the essential criteria for inhibition, other nonspecific interaction with α-glucosidase have also been shown to give false positive results [13].

Despite the risks of false positive results, the standard practice in screening for α-glucosidase inhibitors have so far been based on either affinity (e.g. in ligand fishing) or inhibition (e.g. in high-resolution inhibition profiling) alone. In order to achieve an ideal screening with minimized risk of false positive resultss, we propose a combination of the two techniques, *i.e.*, high-resolution inhibition profiling and ligand fishing, for identification of active constituents with both high binding affinity and high inhibitory activity. In the current study, we present the first example of such combination for identification of α-glucosidase inhibitory ligands in a crude extract of *Ginkgo biloba* - one of the oldest living plant species with proven α-glucosidase inhibitory activity [14].

2. Experimental Section

2.1. Chemicals

Dimethyl sulfoxide, NaH_2PO_4, Na_2HPO_4, pyridine (99.8%), hydroxylamine hydrochloride, sodium cyanoborohydride, ammonium acetate, methanol, acetonitrile, acarbose, *p*-nitrophenyl α-D-glucopyranoside (*p*-NPG), and α-glucosidase type I (EC 3.2.20, from *Saccharomyces cerevisiae*, lyophilized powder) were obtained from Sigma-Aldrich (St. Louis, MO, USA). BcMag aldehyde-activated magnetic beads (lyophilized powder, 1 μm) and long-arm aldehyde-activated magnetic beads (lyophilized powder, 1μm) were purchased from Bioclone (San Diego, CA, USA). Water was purified by deionization and 0.22 μm membrane filtration using a Millipore system (Billerica, MA, USA), and all other solvents were analytical grade. Formic acid was purchased from Merck (Darmstadt, Germany). HPLC-grade acetonitrile and methanol were obtained from VWR International (Fontenay-sous-Bois, France).

2.2. Plant material and extraction.

Dried leaves of *Ginkgo biloba* were ground, and 45 g of this material was extracted with 900 mL of ethyl acetate under sonication for two hours. This yielded 2.45 g of crude extract after evaporation of the ethyl acetate. The dark viscous crude extract was resuspended in MeOH/H_2O (v/v 9:1) and extracted with low boiling petroleum ether (v/v 2:1.5) to provide a defatted crude extract. The methanol fraction was dried using rotatory evaporation at 45 °C and stored in the freezer until use. Crude extract samples for bioassays as well as for HPLC-HRMS analysis were prepared in methanol at concentrations of 20 mg/mL and centrifuged for 3 min at 10,000 rpm before use.

2.3. Preparation of α-glucosidase *N*-terminus coupled magnetic beads.

Immobilization of α-glucosidase was performed using a previously published protocol with slight modifications [9]. In brief, BcMag aldehyde-activated magnetic beads and long-arm aldehyde-activated magnetic beads (30 mg) was suspended in 1 mL of coupling buffer and vigorously vortexed for 3 minutes. The aldehyde-activated magnetic beads were magnetically separated from the supernatant using a magnetic separator (Dynal MPC-S) and washed with 3 × 1 mL of coupling buffer (10 mM aqueous pyridine, pH 6.0). An α-glucosidase (94 units/mg) solution with a concentration of 4.5 mg/mL was prepared in coupling buffer, and 1 mL of this solution was added to the aldehyde-activated beads. The mixture was shaken gently at room temperature for 1 day. After removal of the supernatant, the beads were resuspended in 1 mL end-capping solution (100 mM hydroxylamine in coupling buffer containing 2.5% sodium cyanoborohydride), and incubated for an additional 18 hours. After magnetic separation, the supernatant was discarded and the α-glucosidase *N*-terminus coupled to short-arm ($AG_{NTC\text{-}3}MB$) and long-arm ($AG_{NTC\text{-}21}MB$) aldehyde-activated magnetic beads were washed with 3 × 1 mL of assay buffer (10 mM ammonium acetate, pH 7.4) and stored in 1 mL of the same buffer at 4 °C.

2.4. Fourier-transform infrared (FTIR) microscopy.

Aldehyde-activated magnetic beads and long-arm aldehyde-activated beads without immobilized enzyme as well as $AG_{NTC\text{-}3}MB$ and $AG_{NTC\text{-}21}MB$ were analyzed using FTIR. Thin films of magnetic beads, approximately 10 μg, were deposited on IR-transparent BaF_2-slides. Spectra of the thin films were acquired in the spectral range from 4000 to 750 cm^{-1} using a Perkin Elmer Spotlight 400 FTIR microscopy system with a resolution of 4 cm^{-1}. Before measurement of each sample, an empty background of the BaF_2-slide was collected (same settings) to account for water vapour and CO_2

level. From each sample, a total of three spectra were acquired and averaged from three different locations on the film.

2.5. Immobilized enzyme activity studies.

For both $AG_{NTC\text{-}3}MB$ and $AG_{NTC\text{-}21}MB$, two sets of samples (1.2 mg each) were prepared in 1.5 mL Eppendorf tubes. One set was suspended in 100 μL of assay buffer, whereas the other set was suspended in 100 μL of assay buffer containing 10 mM acarbose. To all solutions, 100 μL of 10 mM *p*-NPG was added, and the resulting mixture was incubated for 1 hour at room temperature. After magnetic separation, the supernatant was collected and the absorbance at 405 nm measured using a SPECTROstar Nano spectrophotometer (BMG labtech, Offenburg, Germany). Aldehyde-activated magnetic beads and long-arm aldehyde-activated beads (1.2 mg each) without immobilized enzyme were analyzed in a similar way and used as blank controls for $AG_{NTC\text{-}3}MB$ and $AG_{NTC\text{-}21}MB$, respectively.

2.5. Scanning electron microscopy (SEM) characterization of magnetic beads

Scanning electron microscopy was conducted on freeze-dried samples of magnetic beads with C-3 and C-21 linkers, with and without immobilized α-glucosidase. The samples were sputter-coated with 6 nm gold using a Leica EM ACE200 vacuum coater (Leica Microsystems, Wetzlar, Germany), and focused ion beam SEM images were acquired using a Quanta FEG 3D instrument (Thermo Scientific, Waltham, MA, USA).

2.6. Ligand fishing of artificial test mixture and *Ginkgo biloba* extract.

For both the artificial test mixture and crude *G. biloba* extract, two parallel ligand-fishing experiments with $AG_{NTC\text{-}3}MB$ and $AG_{NTC\text{-}21}MB$ were performed, using 10 min incubation time

according to the previously performed optimization experiments [9]. The artificial test mixture consisting of gallic acid, L-trytophan, polydatin, and quercetin (0.5 mM each) was prepared in assay buffer (S_0). 600 μL of this mixture was added 10 mg of the functionalized magnetic beads. The resulting suspension was incubated for 10 min at room temperature. The supernatant (S_1) was collected following a magnetic separation, and the beads were washed with 3 × 400 μL of assay buffer (S_2-S_4). Finally, the beads were eluted with 3 × 400 μL of 90% MeOH (S_5-S_7).

All solutions from the ligand-fishing experiment, S_0-S_7, were subjected to chromatographic analysis using an Agilent 1100 series instrument (Santa Clara, CA) equipped with a G1311A quaternary pump, a G1379A degasser, a G1316A thermostatted column compartment, a G1315B photodiode-array detector, a G1329A high-performance auto sampler, and a G244A ion trap mass spectrometer. Mass spectra were acquired in positive ion mode, using a drying temperature of 350 °C, a nebulizer pressure of 40 psi, and a drying gas flow of 10 L/min. Separation was performed using a reversed-phase Luna C_{18}(2) column (Phenomenex, 150 × 4.6 mm i.d., 3 μm particles, 100 Å pore size) maintained at 40 °C. The aqueous eluent (A) consisted of water/acetonitrile (95:5, v/v) and the organic eluent (B) consisted of water/acetonitrile (5:95, v/v); both acidified with 0.1% formic acid. The eluent flow rate was maintained at 0.5 mL/min using the following gradient elution profile: 0 min, 0% B; 30 min, 100% B; 35 min, 100% B; 37 min, 0% B. The chromatography and mass spectrometry modules were controlled by ChemStation ver. B.01.03 (Agilent Technologies, Santa Clara, CA) and Bruker TrapControl ver. 6.1 (Bruker Daltonik, Bremen, Germany), respectively. Data processing was performed using Bruker DataAnalysis ver. 4.0 software (Bruker Daltonik, Bremen, Germany). For *G. biloba*, a solution of the crude ethyl acetate extract (0.625 mg/mL; S_0) was prepared in NH_4OAc buffer containing 5% methanol, and 600 μL of this solution was subjected to ligand fishing and chromatographic analysis using the procedure described above.

2.7. High-resolution α-glucosidase inhibition profiles.

For the high-resolution inhibition profiles, chromatographic separation was performed with an Agilent 1200 series instrument (Santa Clara, CA) consisting of a G1311A quaternary pump, a G1322A degasser, a G1316A thermostatted column compartment, a G1315C photodiode-array detector, a G1367C high performance auto sampler, and a G1364C fraction collector, all controlled by Agilent ChemStation ver. B.03.02 software and equipped with a reversed-phase Luna C_{18}(2) column (Phenomenex, 150 × 4.6 mm i.d., 3 μm particles, 100 Å pore size) maintained at 40 °C. The aqueous eluent (A) consisted of water/acetonitrile (95:5, v/v) and the organic eluent (B) consisted of water/acetonitrile (5:95, v/v); both acidified with 0.1% formic acid. The eluent flow rate was maintained at 0.5 mL/min (for analytical-scale separation) or 20 mL/min (for preparative-scale separation); with the following gradient elution profile: 0 min, 40% B; 25 min, 80% B; 30 min, 100% B; 35 min, 100% B; 37min, 40% B, and 8 min of equilibration. The eluate from 8 to 28 min was fractionated into one 96-well microplate and the solvent was evaporated using an SPD121P Savant SpeedVac concentrator (Thermo Scientific) equipped with an OFP400 oil free pump and a RVT400 refrigerated vapor trap. The α-glucosidase inhibitory activities of the fractions were determined according to the previously reported procedure [3]. In brief, the α-glucosidase inhibition assay was performed in 0.1 M sodium phosphate buffer (pH 7.5) containing 0.02% sodium azide. Solutions of α-glucosidase (2.0 U/mL) and *p*-NPG (10 mM) were prepared in the above buffer (pH 7.5). The contents in all wells were dissolved in 100 μL of 0.1 M sodium phosphate buffer (pH 7.5, 0.02% sodium azide) containing 10% DMSO and 80 μL of α-glucosidase solution in phosphate buffer (2.0 U/mL) was added. After incubation at 28 °C for 10 min, 20 μL *p*-NPG (10 mM in phosphate buffer) were added to give a final volume of 200 μL. Enzyme inhibition was determined by measuring the absorbance of the 4-nitrophenol cleavage product at 405 nm for 35 min using a Thermo Scientific

Multiskan FC microplate photometer (Thermo Scientific, Waltham, MA, USA) controlled by SkanIt ver. 2.5.1 software. Cleavage rates in each well were plotted against their respective retention times to provide the high-resolution α-glucosidase inhibition profile (biochromatogram).

2.8. Isolation and structure determination of active compounds.

Separation of *G. biloba* extracts was performed by preparative-scale HPLC with an Agilent 1100 series instrument (Santa Clara, CA, USA) consisting of a quaternary pump, a degasser, a thermostatted column compartment, a photodiode-array detector, and a high-performance auto sampler, all controlled by Agilent ChemStation ver. B.01.01 software and equipped with a reversed-phase Luna C_{18}(2) column (Phenomenex, 250 × 21.2 mm, 5 μm particles, 100 Å pore size) maintained at room temperature. The flow rate (with solvents as described above) was maintained at 20 mL/min, with the following gradient elution profile: 0 min, 40% B; 25 min, 80% B; 30 min, 100% B; 35 min, 100% B; 37min, 40% B, and 8 min of equilibration. 900 μL of a 40 mg/mL solution of crude extract was injected eight times and peaks were collected manually. The fractions were evaporated to dryness under reduced pressure at 40 °C on a Buchi evaporator (Buchi, Flawil, Switzerland). The isolated compounds were analyzed by LC-HRMS using the above-mentioned 1200 Agilent chromatograph hyphenated with a Bruker micrOTOFQ II mass spectrometer equipped with an electrospray ionization (ESI) interface and controlled by Bruker Hystar software version 3.2 (Bruker Daltonik, Bremen, Germany). NMR experiments were recorded with a Bruker Avance III instrument (^{1}H resonance frequency of 600.13 MHz) at 300 K, using DMSO-d_6 as solvent. ^{1}H and ^{13}C chemical shifts were referenced to the residual solvent signal at δ 2.50 and 39.5 ppm. NMR data processing was performed using Bruker Topspin version 3.2 software.

3. Results and discussion

The α-glucosidase enzyme was covalently coupled to magnetic beads using 3-carbon and 21-carbon aliphatic chains as linkers, resulting in short-arm ($AG_{NTC\text{-}3}MB$) and long-arm ($AG_{NTC\text{-}21}MB$) α-glucosidase *N*-terminus coupled magnetic beads, respectively. Both sets of magnetic beads were characterized with FTIR and SEM, and assessed for their inherent hydrolytic activity and fishing efficiency. Ligand-fishing experiments were performed with a test mixture as well as a crude extract of *Ginkgo biloba*. To evaluate the inhibitory activity of the fished-out ligands, *i.e.*, the ligand-containing fraction, a complementary high-resolution inhibition profiling experiment was performed with *G. biloba* crude defatted extract. After targeted isolation, α-glucosidase inhibitory ligands were identified based on HRMS and NMR analysis.

3.1. Synthesis and characterization of α-glucosidase immobilized magnetic beads.

Enzymes can be immobilized via covalent bonds and via weaker non-covalent interactions, but since the former approach is superior in terms of stability, the latter approach was not pursued in this study. The *N*-terminus of the α-glucosidase enzyme was immobilized onto the surface of silica-based superparamagnetic beads activated with an aldehyde functional group (Figure 1). The unbound aldehyde terminals were end-capped with hydroxylamine to minimize non-specific interactions and imines were reduced to the corresponding amines for improved stability at higher pH. Two sets of beads were synthesized using long-arm (*i.e.*, 21-carbon linkers) or short-arm (*i.e.*, 3-carbon linkers) aldehyde activated magnetic beads as solid support.

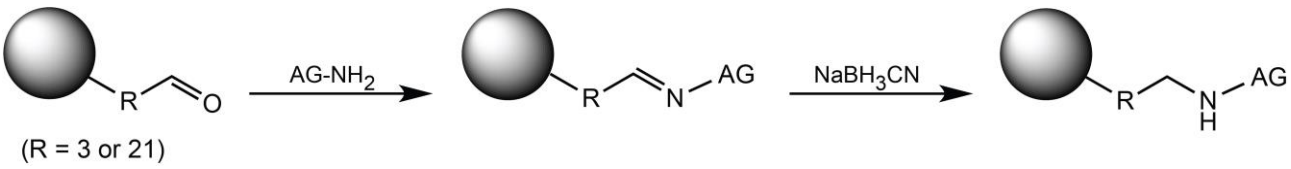

Figure 1. Synthesis of α-glucosidase *N*-terminus coupled magnetic beads by Borch reductive amination.

The resulting immobilized enzymes on short-arm ($AG_{NTC\text{-}3}MB$) and long-arm ($AG_{NTC\text{-}21}MB$) supports were characterized using FTIR microscopy. As shown in Figure 2, the FTIR spectra of both $AG_{NTC\text{-}3}MB$ (grey line) and $AG_{NTC\text{-}21}MB$ (black line) showed strong vibrational bands at 1658 cm^{-1} and 1524 cm^{-1} compared to non-functionalized magnetic beads with 21-carbon (black dotted line) and 3-carbon (grey dotted line) linkers. These correspond to amide-I and amide-II bands, respectively, of the immobilized α-glucosidase, which confirmed the successful immobilization of the enzyme on the solid support. A pronounced difference between the long- and short-arm beads was observed at 2850-2950 cm^{-1}, which corresponds to the relatively stronger C-H stretching band of the aliphatic chain of the long-arm beads [15-16].

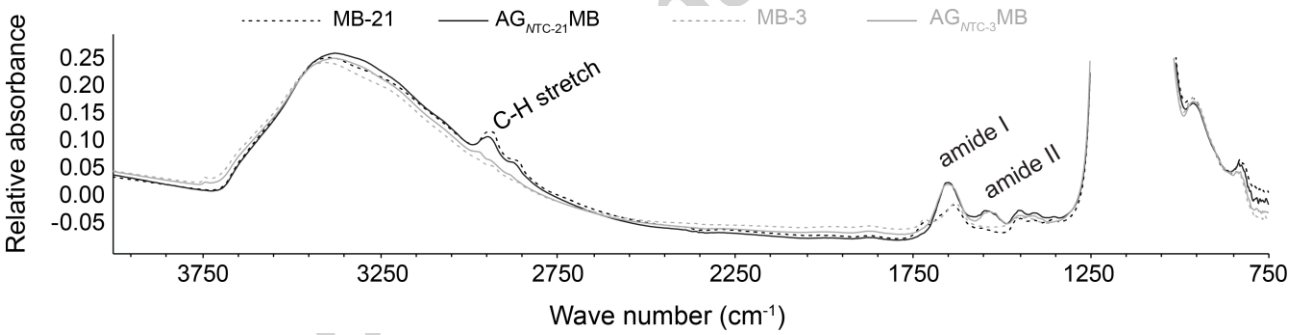

Figure 2. FTIR spectra of long-arm magnetic beads (MB-21), short-arm magnetic beads (MB-3), and α-glucosidase *N*-terminus coupled magnetic beads with short-arm ($AG_{NTC\text{-}3}MB$) and long-arm ($AG_{NTC\text{-}21}MB$) linkers.

Both nonfunctionalized magnetic beads with 3-carbon and 21-carbon linkers as well as $AG_{NTC\text{-}3}MB$ and $AG_{NTC\text{-}21}MB$ were investigated with scanning electron microscopy. The results are shown in

Supplementary data Figure S1, and for all four categories of beads, very irregular shapes and granulated surfaces are observed. However, there are no clear differences between beads with and without immobilized α-glucosidase or between beads with 3-carbon linkers and 21-carbon linkers.

The catalytic activity of $AG_{NTC\text{-}3}MB$ and $AG_{NTC\text{-}21}MB$ was assessed by measuring absorbance of the hydrolysis product *p*-nitrophenolate (*p*-NP) after one hour. The results showed that the hydrolytic activity of $AG_{NTC\text{-}21}MB$ was approximately two-fold higher than that of $AG_{NTC\text{-}3}MB$ (Figure 3). This could be due to the higher hydrodynamic volume of the long-arm beads, providing larger surface area for immobilization of a higher number of catalytically active enzymes. A similar observation was reported by Wang et al., where an increase in hydrodynamic size due to longer linkers (*i.e.*, C_{18}-Fe_3O_4 > C_8-Fe_3O_4 > C_3-Fe_3O_4 > Fe_3O_4), was shown to increase the activity of immobilized lipases [16]. The longer distance between the magnetic bead and the immobilized enzyme may also prevent conformational changes and/or reduced accessibility to the enzyme's binding site - which is a potential drawback of immobilizing enzyme with a short linker. It is also possible that the immobilization is less efficient with the shorter linker, *i.e.*, causing strict requirements for the distance from the enzyme's *N*-terminus to the magnetic bead. This is plausible, because C_8 and C_{18} modified magnetic beads with a higher surface area have been used to accumulate low-abundance peptides effectively [17,18].

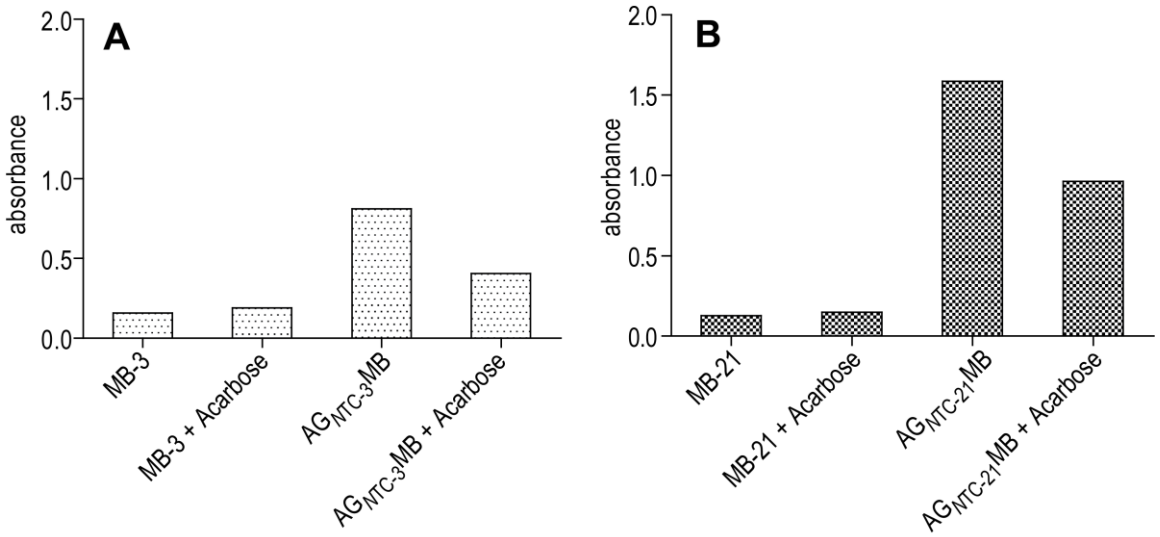

Figure 3. Enzymatic activity of short-arm (**A**) and long-arm (**B**) magnetic beads. In each case four different measurements were performed. MB-3/21: activity of free magnetic beads without immobilized enzyme. MB-3/21 + acarbose: activity of free magnetic beads without immobilized enzyme in the presence of 10 mM acarbose. $AG_{NTC-3/21}MB$: activity of free magnetic beads with immobilized enzyme. $AG_{NTC-3/21}MB$ + acarbose: activity of free magnetic beads with immobilized enzyme in the presence of 10 mM acarbose.

In addition to measuring the catalytic activity, interaction of the immobilized enzymes with an inhibitory ligand was evaluated (Figure 3). Thus, percentage enzyme inhibition in the presence of 10 mM of the competitive inhibitor acarbose was calculated using the following equation:

$$\% \text{ inhibition} = 1 - (A_{acarbose} - A_{blank} / A_{control} - A_{blank'})$$

where A_{blank} is the absorbance of magnetic beads with acarbose, $A_{blank'}$ is the absorbance of aldehyde-activated magnetic beads, $A_{acarbose}$ is the absorbance of α-glucosidase *N*-terminus coupled magnetic beads, substrate and acarbose, and $A_{control}$ is the absorbance of α-glucosidase *N*-terminus

coupled magnetic beads and substrate. Acarbose showed 66.7% inhibition of $AG_{NTC\text{-}3}MB$ and 44.1% inhibition of $AG_{NTC\text{-}21}MB$, and this confirms accessible ligand binding sites of immobilized α-glucosidase. The results of the above studies demonstrate that the enzymatic activity of α-glucosidase was maintained after immobilization.

3.2. Stability after reuse of α-glucosidase immobilized magnetic beads.

The recent developments in enzyme immobilization have revealed that immobilization offers many advantages compared to working with enzymes in solution [19]. Especially important is the possibility of multiple reuses of immobilized enzymes, which makes experiments with expensive enzymes economically more feasible. Thus, the enzymatic activity was measured during multiple reuse experiments with α-glucosidase *N*-terminus coupled magnetic beads (Figure 4). The enzymatic activities decreased to 83% and 84% for $AG_{NTC\text{-}3}MB$ and $AG_{NTC\text{-}21}MB$, respectively, when they were used for the second time. The enzymatic activity decreased only slightly in each of the subsequent six reuse-experiments, and enzymatic activities corresponding to 47% and 58% of the initial enzymatic activity were observed after eight reuse-experiments with $AG_{NTC\text{-}3}MB$ and $AG_{NTC\text{-}21}MB$, respectively.

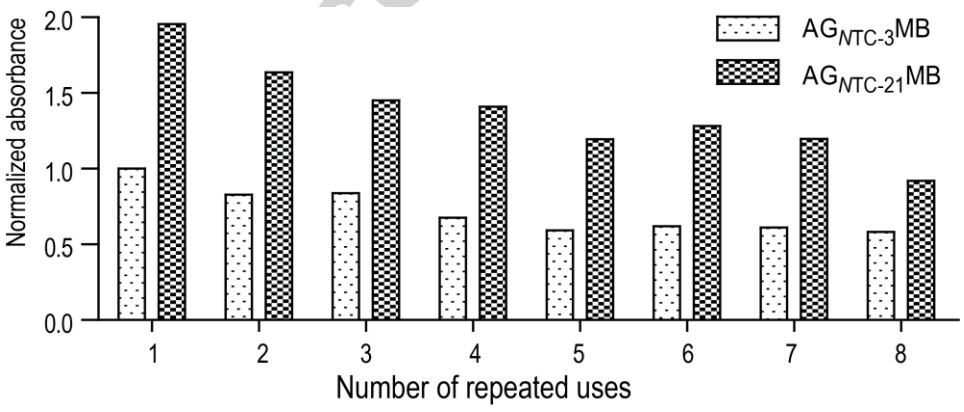

Figure 4. Enzymatic activity measured after successive reuse of $AG_{NTC\text{-}3}MB$ and $AG_{NTC\text{-}21}MB$.

Mamoru and co-workers have previously reported that the activity of immobilized *Pseudomonas fluorescens* lipase decreased to 65% when it was used repeatedly 8 times in a transesterification reaction, which is in the same range as shown in this study [20]. One probable reason for the decrease in enzymatic activity could be build-up of enzyme inhibitors from the enzymatic process, which is classified as build-up of an inhibitory microenvironment around the enzyme [19]. The decrease in enzymatic activity could also be related to loss of particles from the magnetic beads during ligand-fishing experiments, which results in a decreased amount of immobilized enzyme in the subsequent experiments [20].

3.3. Ligand fishing and high-resolution inhibition profile with artificial test mixture.

Ligand-fishing efficiency of $AG_{NTC\text{-}3}MB$ and $AG_{NTC\text{-}21}MB$ was compared using an artificial test mixture consisting of equimolar amounts of the α-glucosidase inhibitor quercetin and the non-inhibitory compounds gallic acid, L-tryptophan, and polydatin. Before performing ligand-fishing, a high-resolution inhibition profile of the artificial mixture was constructed (Figure 5).

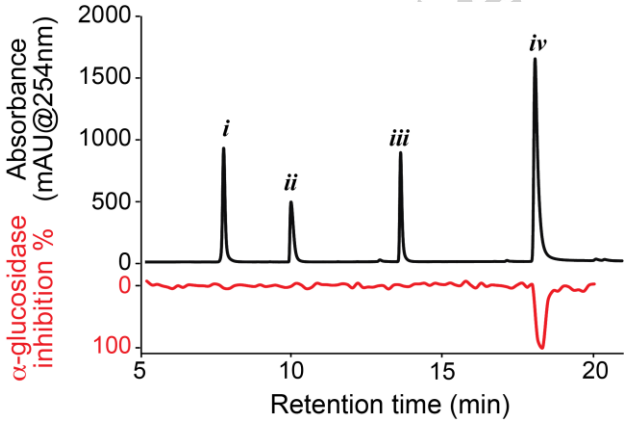

Figure 5. High-resolution α-glucosidase inhibition profile of an equimolar mixture of gallic acid (***i***), L-tryptophane (***ii***), polydatin (***iii***) and quercetin (***iv***).

This confirms that only the three compounds are well-separated with the used chromatographic method, and that only quercetin is detected as an α-glucosidase inhibitory compound. The artificial mixture was thereafter subjected to ligand fishing with $AG_{NTC-3}MB$ and $AG_{NTC-21}MB$. After incubation of the test mixture (S_0) with the magnetic beads, the supernatant (S_1) was removed, and low-affinity ligands were washed off three times with assay buffer (S_2-S_4), before high-affinity binders were eluted using 90% methanol (S_5-S_6). Chromatographic analyses of all solutions (S_0-S_7) are shown in Figure 6. From comparison of the loading solution (S_0) and the first elution (S_5), it was observed that quercetin, *i.e.* the only a-glucosidase inhibitor in the mixture, was selectively fished out using $AG_{NTC-3}MB$. However, in the case of $AG_{NTC-21}MB$, significant amounts of polydatin, *i.e.*, a relatively apolar compound with no α-glucosidase inhibitory activity, was detected in the elution solution (S_5). Such false positive results from ligand-fishing experiments could potentially be due to non-specific binding to the immobilized enzyme or to the long-arm aliphatic linker. Since polydatin was not fished out using $AG_{NTC-3}MB$, the observed non-specific binding in the case of $AG_{NTC-21}MB$ is likely due to hydrophobic interaction of this relatively apolar compound with the long-arm aliphatic linker. Despite the high fishing efficiency of both $AG_{NTC-3}MB$ and $AG_{NTC-21}MB$ shown in these proof-of-concept experiments, the potential risk of detecting non-specific binders was also demonstrated and should be kept in mind at all times.

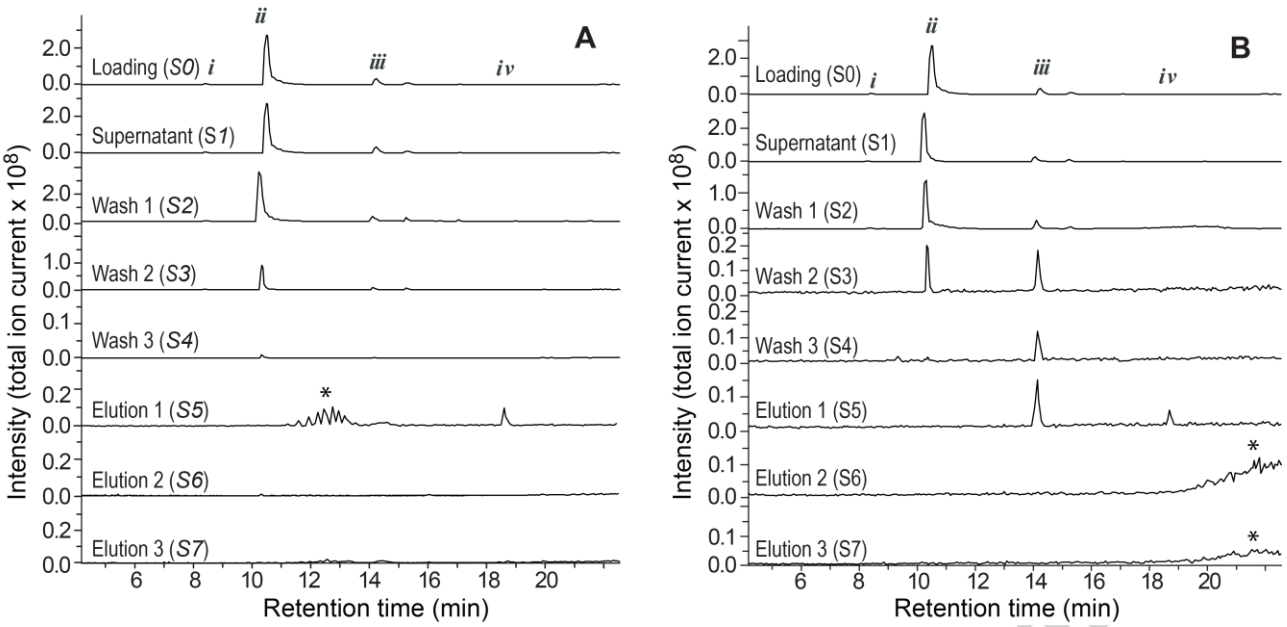

Figure 6. Overlaid base peak chromatograms of different solutions (S_0-S_7) from ligand-fishing experiments using $AG_{NTC\text{-}3}MB$ (**A**) and $AG_{NTC\text{-}21}MB$ (**B**). The ligand-fishing experiments were performed with an artificial test mixture containing equimolar concentrations of gallic acid (***i***), L-tryptophan (***ii***), polydatin (***iii***), and quercetin (***iv***). Note the different TIC intensity scales. * = impurities.

3.4. Ligand fishing with *Ginkgo biloba* crude extract.

In addition to the artificial test mixture, ligand fishing was also performed with a crude ethyl acetate extract of *G. biloba*. *G. biloba* has previously been shown to possess strong α-glucosidase inhibitory activity [21]. The ligand-fishing experiment with $AG_{NTC\text{-}3}MB$ resulted in five peaks (*i.e.*, peaks *2*, *6*, and *7*, and co-eluting peaks *12a* and *12b*) being identified as α-glucosidase ligands based on the UV chromatogram of the first elution fraction (S_5) upon 10-times magnification of the UV chromatogram (Figure 7A). In contrast, the UV chromatograms of elution fraction S_5 from the ligand-fishing experiment using $AG_{NTC\text{-}21}MB$ resulted in a total of eleven peaks (*i.e.*, peak *1-9* and co-eluting peaks *12a* and *12b*) (Figure 7B) being identified as α-glucosidase ligands. In addition, it

was observed that ligand fishing using $AG_{NTC\text{-}21}MB$ resulted in a significantly higher amount of the four major peaks (i.e., peaks *2*, *6*, *7* and *12a*) in all three elution fractions (S_5-S_7). This shows that the higher enzymatic activity of $AG_{NTC\text{-}21}MB$ compared to $AG_{NTC\text{-}3}MB$ (Figure 3) most likely is related to a larger number of α-glucosidase enzymes immobilized on magnetic beads with 21-arm linkers than magnetic beads with 3-arm linkers.

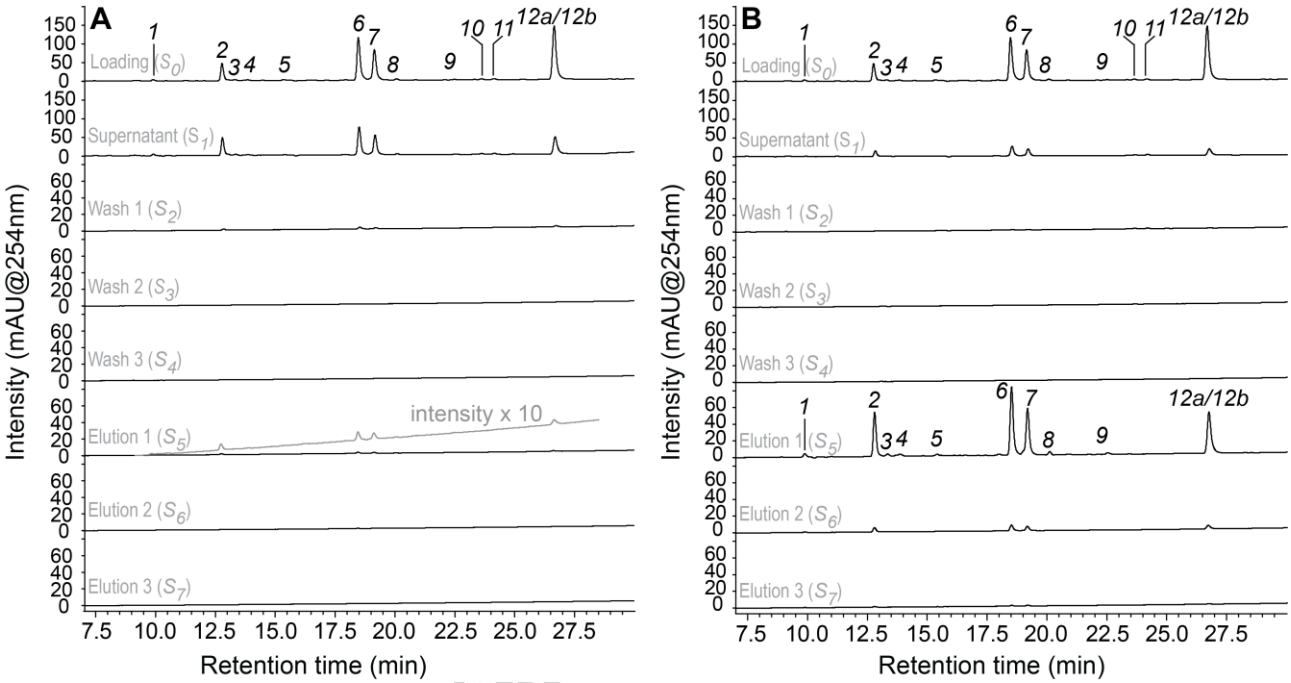

Figure 7. Overlaid UV chromatograms of solutions (S_0-S_7) from ligand-fishing experiments using $AG_{NTC\text{-}3}MB$ (**A**) and $AG_{NTC\text{-}21}MB$ (**B**). The ligand-fishing experiments were performed with ethyl acetate extract of *G. biloba.*

In the case of $AG_{NTC\text{-}3}MB$, no bound ligand was observed after the first elution. The risk of fishing out non-binders (*i.e.*, false positive) due to the hydrophobic interaction from the long-arm aliphatic chain of $AG_{NTC\text{-}21}MB$ was observed in the ligand-fishing experiment with the artificial test mixture (Figure 6). However, it should also be noted that $AG_{NTC\text{-}21}MB$ have shown higher enzymatic activity compared to $AG_{NTC\text{-}3}MB$, which may be explained by a higher number of immobilized

enzymes, which in terms result in higher fishing efficiency. Moreover, previous studies have shown that a therapeutic target immobilized on a long spacer can improve fishing efficiency due to less steric hindrance and more accessible ligand binding pockets [22]. Therefore, before ruling out any of the additional constituents fished out using $AG_{NTC\text{-}21}MB$, a biochromatogram was constructed from high-resolution α-glucosidase inhibition profiling.

3.5. High-resolution α-glucosidase inhibition profiling of *Ginkgo biloba* crude extract.

The principle governing the ligand fishing assay is the binding affinity, typically described by the dissociation constant (K_d) of a molecule towards the immobilized enzyme. High binding affinity of a ligand is a determining factor for its inhibitory activity and have been used to compare compound libraries [10]. However, ligands with high binding affinity can also modulate the enzyme action in other ways than inhibition - *e.g.*, activation. It is therefore crucial to evaluate the α-glucosidase inhibitory activity of ligands identified as binders in the ligand-fishing experiment. Hence, the crude *G. biloba* extract was subjected to high-resolution α-glucosidase inhibition profiling. In addition to complimenting the affinity profile from ligand fishing experiments with inhibition data, high-resolution α-glucosidase inhibition profiling can also serve as a tool to rule out potential false positives. Such false positives in ligand fishing experiments could be a results of none-specific bindings to the solid supports or hydrophobic linkers as demonstrated in section 3.5.

The eluate from 8 to 28 min of an analytical-scale HPLC separation was collected in a 96-well microplate, and the measured α-glucosidase inhibition of each well was plotted against the corresponding retention time to construct a high-resolution α-glucosidase inhibition profile (α-glucosidase biochromatogram) with a resolution of 4.4 data points per min. This high-resolution α-glucosidase inhibition profile was plotted underneath the HPLC chromatogram and used to pinpoint HPLC peaks correlated with α-glucosidase inhibitory activity (Figure 8). The highest inhibition was

observed for the three major peaks, *i.e.*, peaks *6*, *7*, and co-eluting peaks *12a* and *12b*. These peaks were also identified as binders in the ligand-binding experiments using $AG_{NTC\text{-}3}MB$ and $AG_{NTC\text{-}21}MB$, and can therefore be categorized as ligands with inhibitory potential.

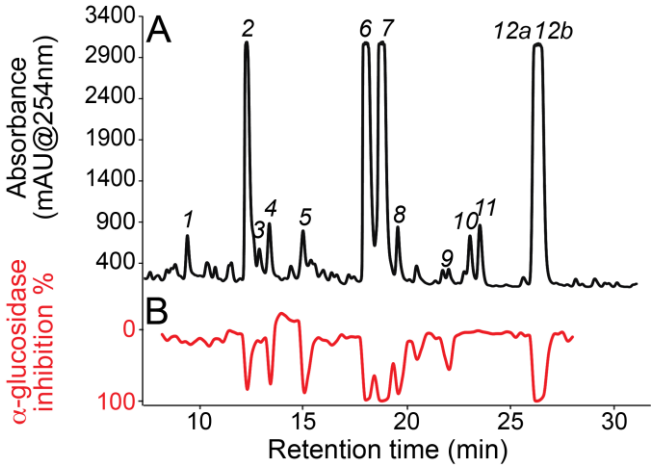

Figure 8. UV chromatogram of crude ethyl acetate of *G. biloba* (**A**) at 254 nm and the corresponding high-resolution α-glucosidase inhibition profile (**B**) from 8 to 28 min.

In addition, substantial inhibition (between 50 to100%) was observed for five peaks, *i.e.*, peaks *2*, *4*, *5*, *8*, and *9*. While the major peak 2 was detected as a binder in both $AG_{NTC\text{-}3}MB$ and $AG_{NTC\text{-}21}MB$, the minor peaks 4, 5, 8 and 9 identified as inhibitors were detected as binders only in the case of $AG_{NTC\text{-}21}MB$ (Figure 7).Results from all the three assays, *i.e.*, ligand fishing using $AG_{NTC\text{-}3}MB$, ligand fishing using $AG_{NTC\text{-}21}MB$, and high-resolution α-glucosidase inhibition profiling, are presented in Table 1. In summary, a total of nine constituents, *i.e.*, peak *2*, *4-9*, and co-eluting peaks *12a* and *12b*, were identified as potential α-glucosidase inhibitory ligands from *G. biloba*. Selection of the true inhibitory ligands was performed based on the combined affinity and inhibition information acquired from the ligand fishing and high-resolution inhibition profiling, respectively.

Table 1. Summary of results from bioactivity profiling of *Ginkgo biloba* extract by ligand fishing (using $AG_{NTC\text{-}3}MB$ and $AG_{NTC\text{-}21}MB$) and high-resolution α-glucosidase inhibition profiling. + indicates the compound being detected in the indicated assay.

Bioactivity profiling	Peaks												
	1	*2*	*3*	*4*	*5*	*6*	*7*	*8*	*9*	*10*	*11*	*12a*	*12b*
Ligand fishing $AG_{NTC\text{-}3}MB$		+				+	+					+	+
Ligand fishing $AG_{NTC\text{-}21}MB$	+	+	+	+	+	+	+	+	+			+	+
High-resolution inhibition profiling		+		+	+	+	+	+	+			+	+
Inhibitory ligands		+		+	+	+	+	+	+			+	+

Peaks identified as binders, inhibitors and inhibitory ligands are marked with '+'

3.6. Structural identification of α-glucosidase inhibitors.

The nine peaks identified as potential α-glucosidase inhibitory ligands were isolated by preparative scale fractionation of crude extract of *G. biloba* and characterized using HRMS and NMR. Substantial amounts could not be isolated for peaks *8* and *12b*, and this led to isolation of seven compounds (compound numbers equal peak numbers): **2** (10.93 mg), **4** (1.42 mg), **5** (1.1 mg), **6** (6.65 mg), **7** (8.74 mg), **9** (1.48 mg), and **12a** (1.13 mg). These compounds were identified as bilobetin (**2**), sotetsuflavone (**4**), sequoiaflavone (**5**), ginkgetin (**6**), isoginkgetin (**7**), 2,3-dihydro-7,4‴-dimethoxy-amentoflavone (**9**), and sciadopitysin (**12a**) (Figure 9B) on the basis of HRMS, ^{1}H-NMR, and/or ^{13}C-NMR data in comparison with literature [23-28]. ^{1}H NMR data of 2,3-dihydro-7,4‴-dimethoxy-amentoflavone is presented here for the first time. Chemical structures of all the identified metabolites are showed in Figure 9B, and retention times, UV maxima, HRMS, and ^{1}H and ^{13}C NMR data are given in Supplementary data Table S1.

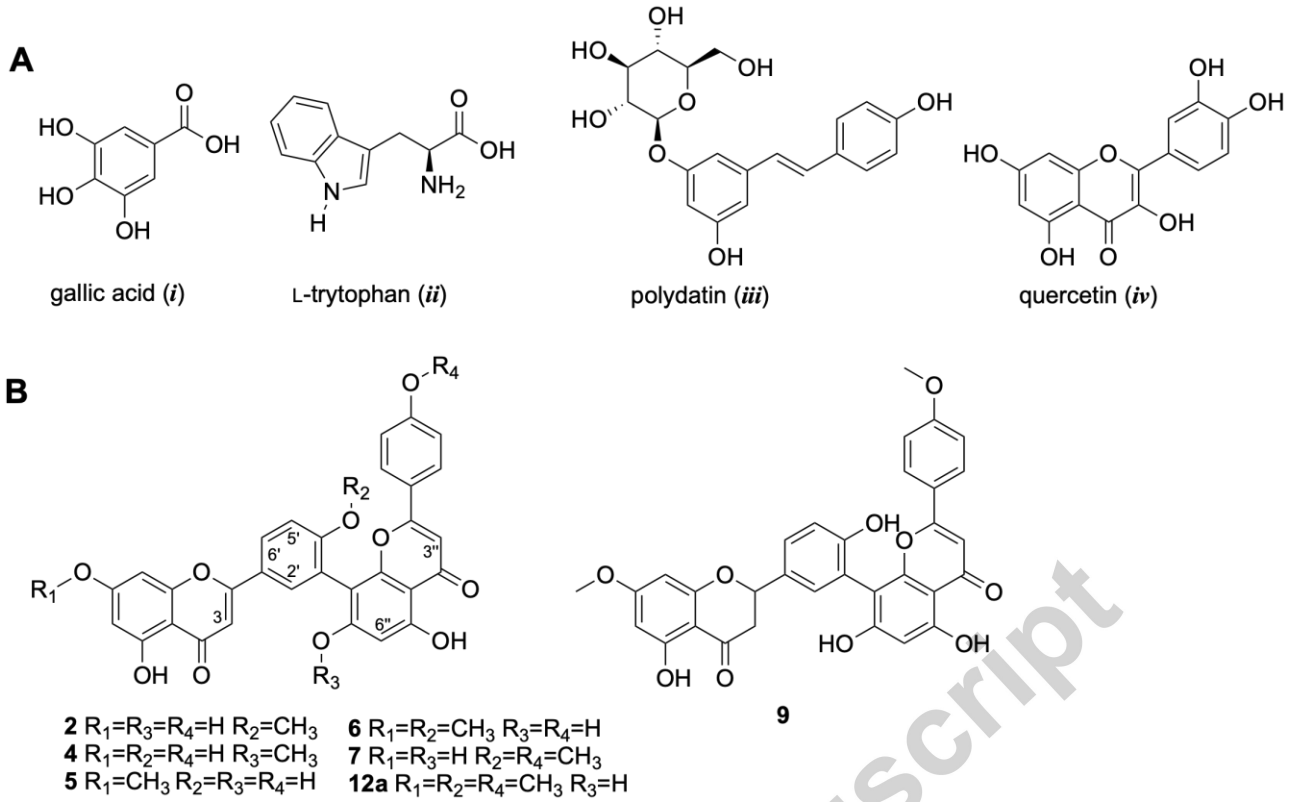

Figure 9. Structures of compounds ***i***, ***ii***, ***iii***, and ***iv*** used in the artificial test mixture for ligand fishing experiments (**A**), and α-glucosidase inhibitory ligands identified from crude ethyl acetate of *G. biloba* (**B**).

Dose-response curves for α-glucosidase inhibitory activity of dilution series of **2**, **4**, **5**, **6**, **7** and **12a** are given in Supplementary Data Figure S2. This provided IC_{50} values of 68.21 ± 1.17 μM for Bilobetin (**2**), 16.35 ± 1.10 μM for Ginkgetin (**6**), 21.13 ± 1.05 μM for isoginkgetin (**7**) and 29.25 ± 1.21 μM for sciadoptysin (**12a**). Sotetsuflavone and sequoiaflavone did not show a sigmoidal inhibition curve in the tested concentration range, and their IC_{50} values are thus higher than 181 μM. It was not possible to isolate enough material for determination of IC_{50} values of the material eluted with peaks *1*, *3*, *8*, *9*, *10*, *11* and *12b*.

Overall, we have demonstrated the potential of combining magnetic ligand fishing and high-resolution inhibition profiling as a powerful screening platform for bioactive constituents in plant extracts. In contrast to the existing strategies of using either one or the other technique, the presented approach provides an opportunity to narrow down the hits, i.e., constituents with presumed bioactivity, by excluding potential false positives from both ligand fishing and high-resolution inhibition profiling. In the case of ligand fishing, such false positive hits can be the result of non-selective interactions between constituents in the mixture and the spacer used for immobilization (see section 3.3). On the other hand, false positive hits from high-resolution inhibition profiling can be the result of e.g. non-specific bioactivities. This phenomenon has previously been shown to result in a false positive activity for tannins, molecules with inherent ability to precipitate target proteins, both when measuring bioactivity of crude extracts and when using high-resolution inhibition profiling [7]. In contrast, the presented combined strategy shown here provides a powerful tool to specifically target bioactive constituents with both specific affinity and activity towards the selected therapeutic target.

4. Conclusions

The α-glucosidase enzyme was immobilized on paramagnetic nanoparticles using short-arm and long-arm aliphatic linkers, and the resulting beads, *i.e.*, $AG_{NTC\text{-}3}MB$ and $AG_{NTC\text{-}21}MB$, were compared for their inherent catalytic activity and ligand fishing efficiency. This showed that enzyme immobilization using the 21-carbon aliphatic linker resulted in higher catalytic activity, but also with an inherent risk of identifying false positive ligands due to hydrophobic interactions with the aliphatic chain. Nevertheless, minor metabolites of *G. biloba* were efficiently fished out using $AG_{NTC\text{-}21}MB$, demonstrating its higher fishing efficiency compared to $AG_{NTC\text{-}3}MB$. The combination with high-resolution bioactivity profiling enabled evaluation of the inhibitory activity

of the binders from the ligand-fishing experiments, and, most importantly, was used to confirm that the binders are true inhibitory ligands. Finally, seven biflavonoids were identified as potential α-glucosidase inhibitory ligands from *G. biloba*. In conclusion, the combined use of the two bioactivity-profiling techniques, *i.e.*, α-glucosidase ligand fishing and high-resolution α-glucosidase inhibition profiling, was shown to be a feasible approach for identification of true α-glucosidase inhibitors while minimizing the risk of identifying false positive hits.

Author Contributions

S.G.W and B.L. contributed equally and have joint first authorship. The manuscript was written through contributions of all authors and all authors have given approval to the final version of the manuscript

Notes

The authors declare no competing financial interests.

Acknowledgements

HPLC equipment used for high-resolution bioactivity profiling was obtained via a grant from The Carlsberg Foundation. The 600 MHz HPLC-HRMS-SPE-NMR system used in this work was acquired through a grant from 'Apotekerfonden af 1991', The Carlsberg Foundation, and the Danish Agency for Science, Technology and Innovation via the National Research Infrastructure funds. We acknowledge the Core Facility for Integrated Microscopy, Faculty of Health and Medical Sciences, University of Copenhagen. Financial support from the Norwegian Research Council through the project PepFishing (261849) and from Aase og Einar Danielsens Fond is greatly acknowledged. The Chinese Scholarship Council is acknowledged for a scholarship to B.L. (Grant Number 201306300102)

Appendix A. Supporting Information

Supplementary data associated with this article can be found in the online version at: TO BE INSERTED

References

[1] L. Ciesla, R. Moaddel, Comparison of analytical techniques for the identification of bioactive compounds from natural products. *Nat. Prod. Rep.* 33 (**2016**) 1131-1145.

[2] O, Potterat, M. Hamburger, Concepts and technologies for tracking bioactive compounds in natural product extracts: generation of libraries, and hyphenation of analytical processes with bioassays. *Nat. Prod. Rep*. 30 (**2013**) 546-564.

[3] J.S. Schmidt, M.B. Lauridsen, L.O. Dragsted, J, Nielsen, D. Staerk, Development of a bioassay-coupled HPLC-SPE-*tt*NMR platform for identification of α-glucosidase inhibitors in apple peel (*Malus* × *domestica* Borkh.). *Food Chem.* 135 (**2012**) 1692-99.

[4] L. Okutan, K.T. Kongstad, A.K Jäger, D. Staerk, High-resolution α-amylase assay combined with high-performance liquid chromatography-solid-phase extraction-nuclear magnetic resonance spectroscopy for expedited identification of α-amylase inhibitors: proof of concept and α-amylase inhibitor in cinnamon. *J. Agric. Food Chem.* 62 (**2014)** 11465-11471.

[5] C. Grosso, A.K. Jäger, D. Staerk, Coupling of a high-resolution monoamine oxidase-A inhibitor assay and HPLC-SPE-NMR for advanced bioactivity profiling of plant extracts. *Phytochem. Anal*. 24 (**2013**) 141-147.

[6] S.G. Wubshet, N.T. Nyberg, M.V. Tejesvi, A.M. Pirttilä, M. Kajula, S. Mattila, D. Staerk, Targeting high-performance liquid chromatography - high-resolution mass spectrometry - solid-phase extraction - nuclear magnetic resonance analysis with high-resolution radical

scavenging profiles - bioactive secondary metabolites from the endophytic fungus *Penicillium namyslowskii*. *J. Chromatogr. A.* 1302 (**2013**) 34-39.

[7] K.T. Kongstad, S.G. Wubshet, A. Johannesen, L. Kjellerup, A.M.L Winther, A.K. Jäger, D. Staerk, High-resolution screening combined with HPLC-HRMS-SPE-NMR for identification of fungal plasma membrane H^+-ATPase inhibitors from plants. *J. Agric. Food Chem.* 62 (**2014**) 5595-5602.

[8] M.A. Arai, E. Kobatake, T. Koyano, T. Kowithayakorn, S. Kato, M.A. Ishibashi, A method for the rapid discovery of naturally occurring products by proteins immobilized on magnetic beads and reverse affinity chromatography. *Chem. Asian. J.* 4 (**2009**) 1802-1808.

[9] S.G. Wubshet, I.M.C. Brighente, R. Moaddel, D. Staerk, Magnetic ligand fishing as a targeting tool for HPLC-HRMS-SPE-NMR: α-glucosidase inhibitory ligands and alkylresorcinol glycosides from *Eugenia Catharinae*. *J. Nat. Prod.* 78 (**2015**) 2657-2665.

[10] L.S. Qing, Y. Xue, W.L. Deng, X. iao, X.M. Xu, B.G. Li, Y.M. Liu, Ligand fishing with functionalized magnetic nanoparticles coupled with mass spectrometry for herbal medicine analysis. *Anal Bioanal. Chem.* 399 (**2011**) 1223-1231.

[11] K. Lourenço Vanzolini, Z. Jiang, X. Zhang, L.C.C. Vieira, A.G. Corrêa, C.L. Cardoso, Q.B. Cass, R. Moaddel, Acetylcholinesterase immobilized capillary reactors coupled to protein coated magnetic beads: a new tool for plant extract ligand screening. *Talanta* 116 (**2013**) 647-652.

[12] M. Yasuda, D.R. Wilson, S.D. Fugmann, R. Moaddel, The synthesis and characterization of SIRT6 protein coated magnetic beads: identification of a novel inhibitor of SIRT6 deacetylase from medicinal plant extracts. *Anal. Chem.* 83 (**2001**) 7400-7407.

[13] K.T. Kongstad, C. Özdemir, A. Barzak, S.G. Wubshet, D. Staerk, Combined use of high-resolution α-glucosidase inhibition profiling and high-performance liquid chromatography-

high-resolution mass spectrometry-solid-phase extraction-nuclear magnetic resonance spectroscopy for investigation of antidiabetic principles in crude plant extracts. *J. Agric. Food Chem.* 63 (**2015**) 2257-2263.

[14] M. Pinto, S. Da, Y.I. Kwon, E. Apostolidis, F.M. Lajolo, M.I. Genovese, K. Shetty, Potential of *Ginkgo Biloba* L. leaves in the management of hyperglycemia and hypertension using in vitro models. *Bioresour. Technol.* 100 (**2009**) 6599-6609.

[15] A. Barth, Infrared spectroscopy of proteins. *Biochim. Biophys. Acta*. 1767 (**2007**) 1073-1101.

[16] J. Wang, G. Meng, K. Tao, M. Feng, X. Zhao, Z. Li, H. Xu, D. Xia, J.R. Lu, Immobilization of lipases on alkyl silane modified magnetic nanoparticles: effect of alkyl chain length on enzyme activity. *PLoS One* 7 (**2012**) e43478.

[17] N. Yao, H. Chen, H. Lin, C. Deng, X. Zhang, Enrichment of peptides in serum by C8-functionalized magnetic nanoparticles for direct matrix-assisted laser desorption/ionization time-of-flight mass spectrometry analysis. *J. Chromatogr. A*. 1185 (**2008**) 93-101.

[18] S. Baumann, U.G. Ceglarek, M. Fiedler, J. Lembcke, A. Leichtle, J. Thiery, Standardized approach to proteome profiling of human serum based on magnetic bead separation and matrix-assisted laser desorption/ionization time-of-flight mass spectrometry. *Clin. Chem*. 51 (**2005**) 973-980.

[19] A.A. Homaei, R. Sariri, F. Vianello, R. Stevanato, Enzyme immobilization: an update. *Chem. Biol.* 6 (**2013**) 182-205.

[20] I. Mamoru, B.X. Chen, E. Masashi, K. Takashi, S. Surekha, Production of biodiesel fuel from triglycerides and alcohol using immobilized lipase. *J. Mol. Catal. B: Enzym*. 16 (**2001**) 53-58.

[21] M.D.S. Pinto, Y.I. Kwon, E. Apostolidis, F.M. Lajolo, M.I. Genovese, K. Shetty, Potential of *Ginkgo Biloba* L. leaves in the management of hyperglycemia and hypertension using in vitro models. *Bioresour. Technol.* 100 (**2009**) 6599-6609.

[22] J. Wang, G. Meng, K. Tao, M. Feng, X. Zhao, Z. Li, H. Xu, D. Xia, J.R. Lu, Immobilization of lipases on alkyl silane modified magnetic nanoparticles: effect of alkyl chain length on enzyme activity. *PLoS One* 7 (**2012**) e43478.

[23] Y.B. Ryu, H.J. Jeong, J.H. Kim, Y.M. Kim, J.Y. Park, D. Kim, T.T.H. Naguyen, S.J. Park, J.S. Chang, K.H. Park, M.C. Pho, W.S. Lee, Biflavonoids from *Torreya nucifera* displaying SARS-CoV $3CL^{pro}$ inhibition. *Bioorg. Med. Chem.* 18 (**2010**) 7940-7947.

[24] K.R. Markham, C. Sheppard, H. Geiger, ^{13}C NMR studies of some natural occurring amentoflavone and hinokiflavone bifavonoids. *Phytochemistry* 26 (**1987**) 3335-3337.

[25] S.H. Li, H.J. Zhang, X.M. Niu, P. Yao, H.D. Sun, H.H.S. Fong, Chemical constituents from *Amentotaxus yunnanensis* and *Torreya yunnanensis*. *J. Nat. Prod.* 66 (**2003**) 1002-1005.

[26] M. Krauze-Baranowska, L. Poblocka, A.A. El-Hela, Biflavones from *Chamaecyparis obtuse*. *Z. Naturforsch.* 60c (**2005**) 679-685.

[27] K.T. Cheng, F.L. Hsu, S.H. Chen, P.K. Hsieh, H.S. Huang, C.K. Lee, M.H. Lee, New constituent from *Podocarpus macrophyllus* var. *macrophyllus* shows anti-tyrosinase effect and regulated tyrosinase-related protein and mRNA in human epidermal melanocytes. *Chem. Pharm. Bull.* 55 (**2007**) 757-761.

[28] M.K. Lee, S.W. Lim, H. Yang, S.H. Sung, H.S. Lee, M.J. Park, Y.C. Kim, Osteoblast differentiation stimulating activity of biflavonoids from *Cephalotaxus koreana*. *Bioorg. Med. Chem. Lett.* 16 (**2006**) 2850-2854.

HIGHLIGHTS

- α-Glucosidase was immobilized on magnetic beads using C-3 and C-21 spacers
- Higher activity and ligand fishing efficiency was observed when using C-21 spacers
- Combining ligand fishing and high-resolution inhibition enabled efficient screening
- Advantage of the combined screening was demonstrated using a test mixture
- A proof-of-concept was successfully conducted on a crude extract of *Ginkgo biloba*